Intracerebral chondroitinase ABC and heparan sulfate proteoglycan glypican improve outcome from chronic stroke in rats

Justin J. Hill[a], Kunlin Jin[a,b], Xiao Ou Mao[a], Lin Xie[a], and David A. Greenberg[a,1]

[a]Buck Institute for Research on Aging, Novato, CA 94945; and [b]Department of Pharmacology and Neuroscience, University of North Texas, Fort Worth, TX 76107

Edited by Solomon H. Snyder, The Johns Hopkins University School of Medicine, Baltimore, MD, and approved April 27, 2012 (received for review April 4, 2012)

Physical and chemical constraints imposed by the periinfarct glial scar may contribute to the limited clinical improvement often observed after ischemic brain injury. To investigate the role of some of these mediators in outcome from cerebral ischemia, we treated rats with the growth-inhibitory chondroitin sulfate proteoglycan neurocan, the growth-stimulating heparan sulfate proteoglycan glypican, or the chondroitin sulfate proteoglycan-degrading enzyme chondroitinase ABC. Neurocan, glypican, or chondroitinase ABC was infused directly into the infarct cavity for 7 d, beginning 7 d after middle cerebral artery occlusion. Glypican and chondroitinase ABC reduced glial fibrillary acidic protein immunoreactivity and increased microtubule-associated protein-2 immunoreactivity in the periinfarct region, and glypican- and chondroitinase ABC-treated rats showed behavioral improvement compared with neurocan- or saline-treated rats. Glypican and chondroitinase ABC also increased neurite extension in cortical neuron cultures. Glypican increased fibroblast growth factor-2 expression and chondroitinase ABC increased brain-derived neurotrophic factor expression in these cultures, whereas no such effects were seen following neurocan treatment. Thus, treatment with glypican or enzymatic disruption of neurocan with chondroitinase ABC improves gross anatomical, histological, and functional outcome in the chronic phase of experimental stroke in rats. Changes in growth factor expression and neuritogenesis may help to mediate these effects.

astrocyte | astrogliosis | glia

Patients who survive an acute stroke are typically left with fixed anatomical deficits and associated functional impairment in the chronic phase of injury, for which few therapeutic options exist. One reason for limited recovery from stroke may be the development of a glial scar at the border between normal and ischemic tissue (1, 2). The glial scar, which contains reactive astrocytes and associated extracellular matrix (ECM) proteins such as chondroitin sulfate proteoglycans (CSPGs) (3, 4), appears to serve a beneficial function in the acute phase of stroke, by confining the lesion and limiting toxic effects on adjacent tissue (5). However, it also inhibits axonal growth and, perhaps, other repair processes (1, 6, 7), thereby interfering with long-term anatomical and functional recovery. Conversely, some ECM proteins, such as the heparan sulfate proteoglycan (HSPG) glypican (8), can stimulate neurite growth after CNS injury (9). The role of these proteins in inhibition of recovery by the postischemic glial scar and the effect of their modification on functional and anatomical outcome from stroke are unknown.

CSPGs, a major constituent of the glial scar (10), exist in several isoforms (11). Despite variations in their core proteins, CSPG isoforms share a conserved glycosaminoglycan side chain, which appears to inhibit axonal migration. CSPGs such as neurocan are powerful inhibitors of axonal growth cones and neurite extension in vitro (11), but this effect can be overcome if CSPGs are degraded by chondroitinase (Ch)ABC, which cleaves glycosaminoglycan side chains (12). ChABC also increases axonal regeneration following nigrostriatal tractotomy (13) and improves nerve regeneration (14) and functional recovery after spinal cord injury (15, 16) in rats in vivo. Like CSPGs, HSPGs are extracellular proteins that exist in several isoforms (17, 18). HSPG isoforms share a conserved glycosaminoglycan side chain, which has more sulfur groups compared with CSPGs. HSPGs appear to up-regulate fibroblast growth factor (FGF)2 and enhance neurogenesis in the olfactory system (19). The role of HSPGs in the chronic phase of the glial scar in stroke is unclear.

Considering the putative role of the glial scar in limiting recovery from stroke and the effectiveness of enzymatic dissolution of the scar in other neuropathological settings, a similar approach might be applicable to the chronic phase of cerebral ischemia. We hypothesized that treatment with ChABC would reduce accumulation of CSPGs such as neurocan in the periinfarct glial scar and improve histological and functional outcome in the chronic phase of stroke following middle cerebral artery occlusion (MCAO) in rats. Furthermore, we hypothesized that treatment with the HSPG glypican would also improve functional and anatomical outcome, whereas the CSPG neurocan would not.

Results

Histology. Brains examined 14 d after MCAO showed cavitary cerebrocortical lesions within the distal middle cerebral artery (MCA) territory (Fig. 1). Immunofluorescence staining demonstrated a band of neurocan immunoreactivity at the margin of these lesions, surrounded by a zone of GFAP-immunopositive hypertrophic astrocytes. Increased glypican immunoreactivity was also observed, with a more diffuse perilesional distribution than that of neurocan. Neither sham-operated rats nor the homologous site in the contralesional hemisphere of rats subjected to MCAO showed neurocan or glypican deposition or astrogliosis.

Microtubule-associated protein (MAP)2 immunohistochemistry was used to probe the effects of neurocan, glypican, and ChABC on neuronal elements in the periinfarct region. Glypican and ChABC increased MAP2 "spot count" by ~175% and ~125%, respectively, in the cortex adjacent to the infarct cavity and including the glial scar (Fig. 2). In contrast, neurocan had no effect compared with controls.

To examine the effect of neurocan, glypican, and ChABC on astrogliosis, tissue was analyzed for the extent of GFAP immu-

Author contributions: J.J.H., K.J., and D.A.G. designed research; J.J.H., X.O.M., and L.X. performed research; J.J.H., K.J., and D.A.G. analyzed data; and J.J.H. and D.A.G. wrote the paper.

The authors declare no conflict of interest.

This article is a PNAS Direct Submission.

[1]To whom correspondence should be addressed. E-mail: dgreenberg@buckinstitute.org.

This article contains supporting information online at www.pnas.org/lookup/suppl/doi:10.1073/pnas.1205697109/-/DCSupplemental.

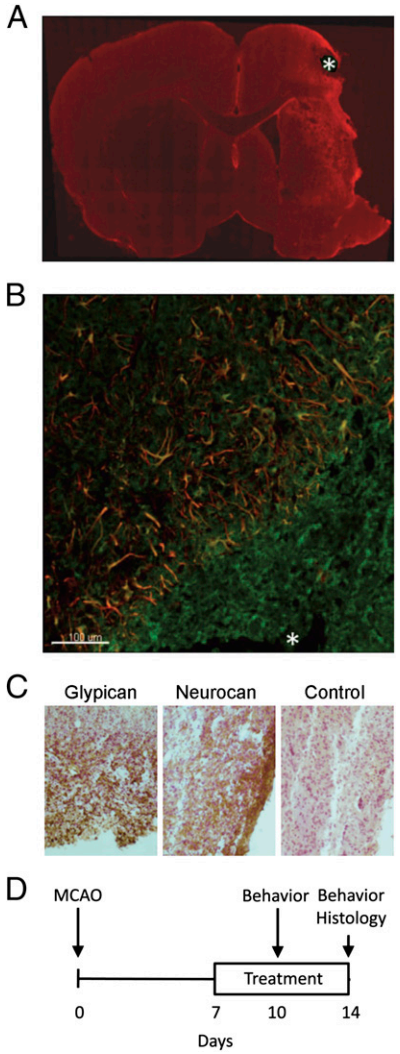

Fig. 1. (*A*) Ischemic rat brain 14 d after MCAO, stained for GFAP (red). Asterisk shows approximate site from which tissue was taken for immunohistochemical studies. (*B*) Scar surrounding infarct cavity (asterisk at bottom) containing CSPG (green), which extends into the surrounding glial scar, as delineated by GFAP-immunoreactive reactive astrocytes (red). (Scale bar: 100 μm.) (*C*) Distribution of glypican (*Left*, brown) and neurocan (*Center*, brown) immunoreactivity in relation to infarct cavity (*Lower Right*) and compared with control section from which primary antibody was omitted (*Right*). Hematoxylin (red) was used to counterstain nuclei. (Magnification, 20×.) (*D*) Timeline of experimental protocol. Rats were treated with PBS, neurocan, glypican, or ChABC on days 7–14 post-MCAO and tested for behavioral and histological outcome on days 10 and 14 post-MCAO.

noreactivity surrounding the infarct cavity. Glypican- and ChABC-treated animals showed ~50% and ~40% respective decreases in thickness of GFAP-immunopositive zone at the periphery of the ischemic lesion (Fig. 2), whereas neurocan-treated rats did not differ from controls in this respect.

Behavior. Behavior was tested at 10 and 14 d after MCAO to evaluate whether neurocan, glypican, or ChABC affected functional outcome (Fig. 3). Compared with PBS-treated controls, glypican- and ChABC-treated rats showed ~70% and ~45% reductions in the number of missteps in the ladder rung walking test at 10 d and ~80% and ~60% decreases in the number of missteps at 14 d, respectively. Forepaw weakness scores in glypican- and ChABC-treated rats were ~25% and ~35% lower at 10 d and ~50% and ~50% at 14 d, respectively. In the cylinder test, ChABC treatment increased touches on the cylinder wall by ~95% at 10 d and ~165% at 14 d, compared with controls, but glypican had no effect. Neurocan had no effect compared with controls in any of the three behavioral tests. No differences was noted between groups pre-MCAO or before the onset of treatment on day 7.

Neuronal Cultures. To evaluate the effects of neurocan, glypican and ChABC on isolated neurons, cortical neurons cultured from embryonic day (E)17 rat cerebral cortex were treated with each protein, at a range of concentrations, from day in vitro (DIV) 0 until DIV 7. Western analysis (Fig. 4) showed that, as anticipated, ChABC reduced neurocan levels. MAP2 expression was increased in ChABC-treated and, to a lesser extent, in glypican-treated cultures. Expression of BDNF and FGF2, which have been implicated in some effects of CSPGs (20, 21) and HSPGs (22, 23) respectively, was examined to determine if these growth factors might be candidate mediators of the ChABC- and glypican-induced increases in MAP2 immunoreactivity. ChABC increased BDNF expression, whereas glypican increased FGF2 expression.

Neurite Growth. We next examined whether treatments that increased MAP2 expression were associated with increased neurite outgrowth, as measured by cresyl violet staining of processes extending across a porous membrane in cell culture (24, 25). ChABC (2 U/mL) increased neurite growth by ~50% and glypican (5 μg/mL) increased growth by ~20% compared with controls, whereas neurocan (5 μg/mL) had no effect (Fig. 5). Neurite growth was unaltered at lower concentrations of these proteins, and cytotoxicity occurred with >10 U/mL ChABC, >100 μg/mL glypican, and >10 μg/mL neurocan.

Discussion

The main findings of this study are that administration of the HSPG glypican or the CSPG (neurocan)-degrading enzyme ChABC, beginning 7 d after MCAO, increases MAP2 immunoreactivity in the periinfarct region, reduces the thickness of the GFAP-immunoreactive glial scar, and improves neurobehavioral outcome in rats. These effects were notable for being observed even though treatment was delayed in onset until 1 wk after MCAO. ChABC and, to a lesser extent glypican, also increased MAP2 immunoreactivity in cortical neuron cultures. This was associated with increased neurite outgrowth and increased expression of BDNF (by ChABC) and FGF2 (by glypican).

These results are consistent with previous studies in other disease models. Intrathecal ChABC enhanced regeneration of dorsal corticospinal tract axons and recovery of fine motor, proprioceptive, and locomotor function after crush injury (15) or transection (16) of the posterior funiculus of the cervical spinal cord in rats. ChABC also stimulated regrowth of tyrosine hydroxylase-positive axons across the lesion site following nigrostriatal tractotomy (13) in rats. In another study, rats given ChABC after cortical impact injury demonstrated increased axonal sprouting in the vicinity of the lesion but little effect on behavioral improvement (26). Finally, intraspinal ChABC given 3 d after an endothelin-induced cortical lesion promoted axonal sprouting from the unaffected toward the affected corticospinal tract and improved sensorimotor recovery in aged rats (27). Other studies have shown effects of ChABC on axonal conduction, synapse formation, cell adhesion, growth factor diffusion, neuronal nets, and inflammation (5, 11, 28, 29). In contrast, one prior study found no effect of ChABC, given as a single intracerebroventricular injection 24 h after neonatal hypoxic–ischemic brain injury in rats, on the wet weight of surviving brain tissue (30).

Reactive astrocytes appear to be the main source of glial scar CSPG following CNS injury (31), but it is not obvious that

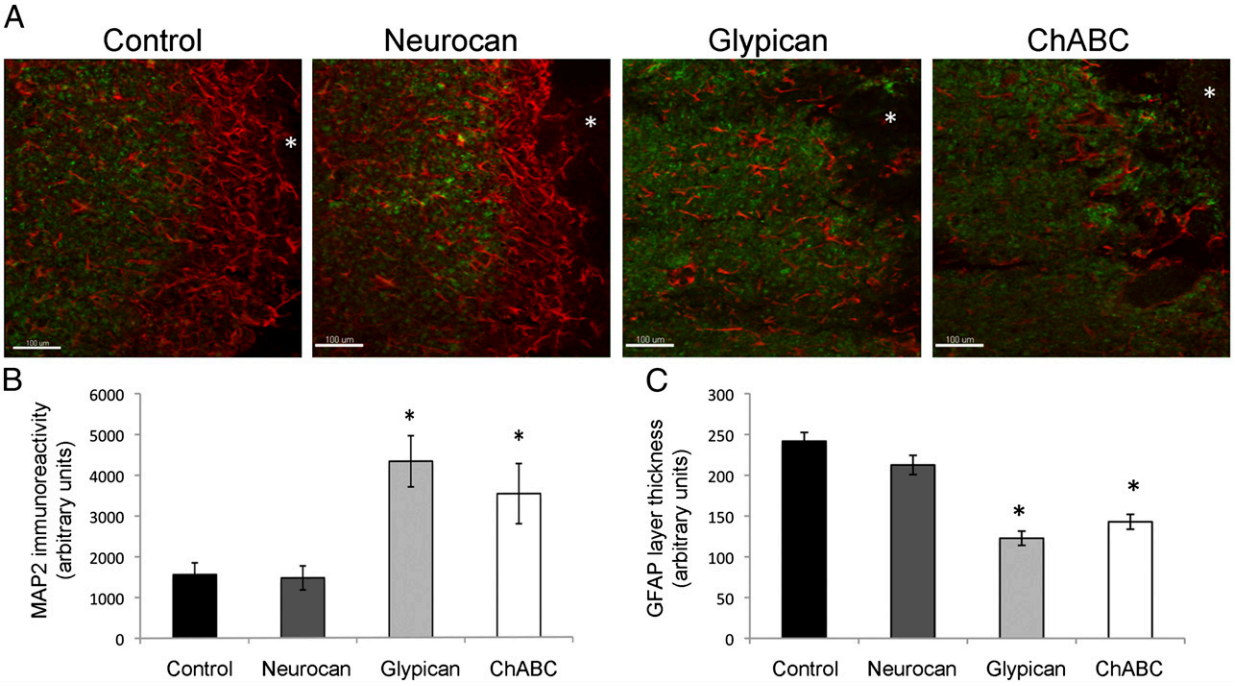

Fig. 2. Representative images (*A*) and quantification of GFAP (*B*, red) and MAP2 (*C*, green) immunoreactivity adjacent to infarct cavity, 14 d after MCAO followed by treatment on days 7–14 with PBS (control), neurocan, glypican, or ChABC. Asterisks in *A* indicate infarct cavity. Asterisks in *B* and *C* indicate significant differences compared with control ($P < 0.05$).

ChABC-induced reduction of CSPG immunoreactivity should also be accompanied by a decrease in astrogliosis, such as we observed. One possible explanation would be interruption by ChABC of a positive-feedback effect of CSPG on astrocyte activation. Of interest, astrocytes express the protein tyrosine phosphatase (PTP)σ receptor (32) that also mediates inhibition of neurite extension by CSPG (33), and PTPσ-knockout mice show developmental abnormalities of GFAP-positive fibers in the spinal cord (34). Moreover, ChABC treatment reduced GFAP reactivity in a study of spinal cord injury in rats (35). Thus, ChABC-induced cleavage of CSPG might reduce glial scar formation not only directly but also by inhibiting astrocytic activation. An altered ratio of neurocan to glypican may also contribute to improvement in glypican-treated rats.

The mechanisms underlying ChABC-induced improvement following stroke may differ from those that operate in spinal cord injury or nigrostriatal tractotomy, where the glial scar presents a physical and chemical barrier to nerve regrowth along preexisting axonal pathways. In contrast, nerve cell bodies (as well as other cell types) are lost in stroke, and recovery appears to involve the formation of new connections that bypass rather than traverse the injury site (36). Such connections might be susceptible to the effects of chemical mediators produced or sequestered by the glial scar, such as growth factors and inflammatory cytokines. We found that ChABC and glypican, which reduced glial scar thickness, improved behavioral outcome after MCAO, and enhanced neurite outgrowth in vitro, also increased expression of BDNF and FGF2, respectively. Of interest, BDNF reduces astrocytosis and CSPG deposition and increases axon growth following spinal cord injury (20), and FGF2 promotes neurite extension in vitro (37).

Repair in the CNS is constrained not only by the glial scar, but also by oligodendrocyte-derived growth-inhibitory molecules, such as Nogo, myelin-associated glycoprotein, oligodendrocyte myelin glycoprotein, semaphorin 4D, and ephrin B3 (2). Like ChABC, antibodies against some of these molecules also produce behavioral improvement in rats after MCAO (38, 39). Whether the effects of ChABC or glypican and such antibodies are additive will be of interest to explore, as will the combined effects of ChABC or glypican and transplantation, which has proved more efficacious than either treatment alone in models of retinal degeneration (40), neonatal hypoxia-ischemia (30), and spinal cord injury (41).

Given that stroke is a leading cause of morbidity and mortality and that, aside from physical and occupational therapy, treatment for the chronic phase is lacking, the ability to achieve improvement following delayed intervention in experimental models is encouraging. This study adds glypican and ChABC to the list of measures, which include growth factors and stem cell administration, that are candidates for such delayed restorative therapy.

Materials and Methods

Middle Cerebral Artery Occlusion. Animal studies were approved by the Buck Institute Institutional Animal Care and Use Committee (IACUC) and conducted according to National Institutes of Health guidelines. Sprague–Dawley rats weighing 250–350 g were maintained on a 12-h sleep/wake cycle with free access to food and water. The MCAO clip model was performed as described previously (42, 43). Isoflurane (4% vol/vol) was used for anesthesia in a mixture of 70% N_2O/30% O_2 and adjusted based on ventilation level and response to forepaw pinch. The core temperature was maintained at 37 °C with a heating blanket and monitored using a rectal thermometer. Betadine was used to create a sterile field. The left common carotid artery (CCA) was permanently occluded with a 6-0 silk suture, and the right CCA was temporarily occluded with a clip. Next, the left temporal muscle was retracted and the cranium overlying the MCA was removed. After exposure of the proximal MCA, an electrocautery was used to permanently occlude the MCA without damage to adjacent tissue. The surgical incision was closed and the animal was placed in a warm cage and allowed to awaken. Buprenorphine and meloxicam were used for postoperative analgesia. After 60 min, the animal was again placed under anesthesia and the clip on the right CCA was removed. Animals were euthanized 14 d after MCAO.

Drug Administration. Seven days after MCAO, a microosmotic pump (Alzet minipump; Model 1007D) was inserted into the infarct cavity, 1.4 mm anterior

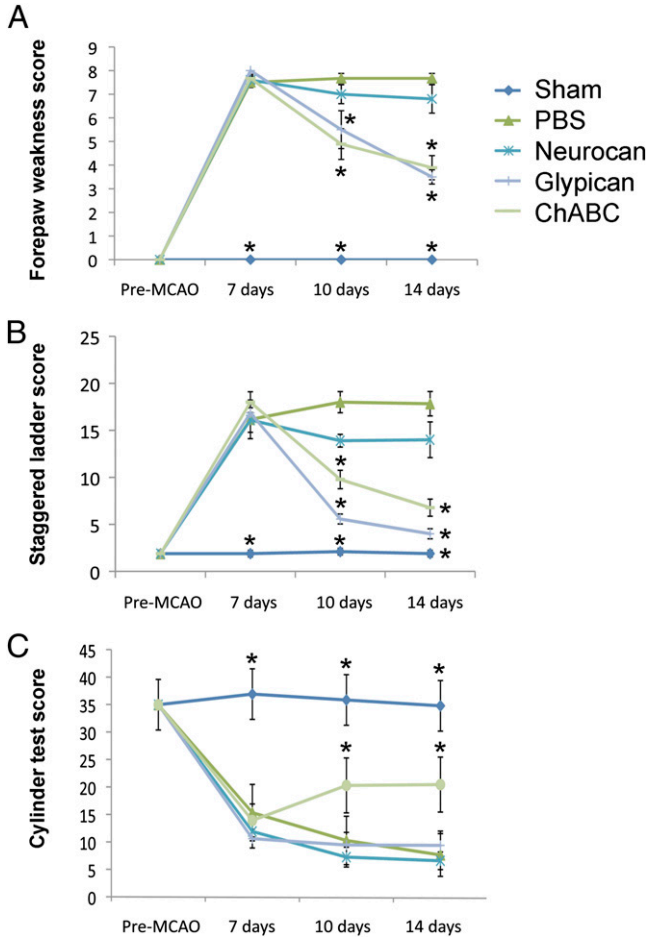

Fig. 3. Forepaw weakness (*A*), staggered ladder (*B*), and cylinder test (*C*) scores before (Pre-MCAO) and 7, 10, and 14 d after MCAO in sham-operated rats and rats treated starting at 7 d post-MCAO with PBS, neurocan, glypican, or ChABC. *$P < 0.05$ compared with PBS treatment.

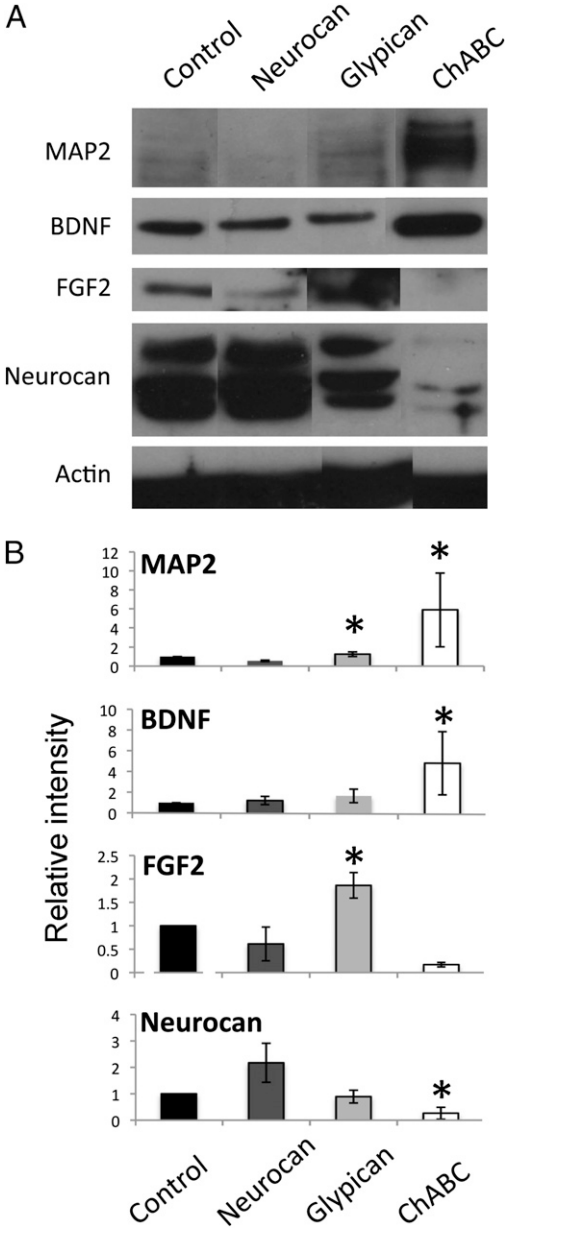

Fig. 4. Western analysis of cortical neuron protein expression. E17 primary cortical neuron cultures were treated from DIV 0–7 with either PBS (control), 5 μg/mL neurocan, 5 μg/mL glypican, or 2 U/mL ChABC. (*A*) Western blots. (*B*) Densitometry measurements normalized to actin, expressed as mean values ± SEM from three experiments. *$P < 0.05$ compared with control.

and 5.5 mm lateral to bregma, under anesthesia as described above. Betadine was used to create a sterile field. After the periosteum was exposed, 30% H_2O_2 was used to further reduce bacterial load. A 0.3-mm dental drill was used to create a burr hole in the skull, and the minipump was fastened to the calvarium with superglue. Meloxicam and buprenorphine were administered for postoperative analgesia. ChABC (9.35 μg total dose; Sigma), neurocan (9.35 μg total dose; Sigma), glypican (9.35 μg total dose; Sigma), or PBS was infused via minipump at 0.5 μL/h for 7 d. Minipumps were numbered and the investigator was blinded to which treatment was delivered. When animals were euthanized, minipumps were inspected to ensure drug delivery.

Immunohistochemistry. Rats were euthanized under anesthesia and perfused with 200 mL of PBS and 200 mL of 4% paraformaldehyde. Tissue was sectioned with a vibratome at a thickness of 50 μm, washed in PBS for 20 min, and permeabilized for 1 h in 0.2% Triton in Tris-buffered saline. Sections were blocked using 5% normal goat serum with 0.2% Triton in Tris-buffered saline for 1 h and incubated with primary antibody in blocking buffer overnight at 4 °C. Sections were then washed for 1 h in PBS containing 0.1% Tween 20 and incubated with secondary antibody in blocking buffer for 1 h at room temperature. After a 1-h wash in PBS, sections were mounted using Prolong Gold with DAPI (Invitrogen). The primary antibodies used were rabbit anti-GFAP (1:1,000; Sigma), mouse anti-neurocan (1:100; Sigma), mouse anti-glypican (1:100; R&D Systems), and mouse anti- MAP2 (1:500; Sigma). Secondary antibodies for immunofluorescence were Alexa Fluor-conjugated donkey anti-mouse or anti-rabbit IgG (1:200; Molecular Probes). Sections were imaged on a laser scanning confocal microscope (LSM 510; Carl Zeiss). For diaminobenzidine (DAB) staining, after incubation overnight with primary antibodies as described above, sections were washed for 1 h in PBS containing 0.1% Tween 20 and incubated with biotinylated anti-mouse IgG secondary antibody (1:200; Vectastain Elite ABC; Vector) in blocking buffer for 1 h at room temperature. Sections were then placed in avidin–peroxidase conjugate (Vector) for 1 h. The horseradish peroxidase reaction was detected with 0.05% DAB and 0.03% H_2O_2. Processing was stopped with H_2O. Sections were counterstained with hematoxylin for 30 s, dehydrated through graded alcohols, cleared in xylene, and cover-slipped in permanent mounting medium (Vector). Sections were imaged using a Nikon E300 epifluorescence microscope. Controls included omitting the primary or secondary antibodies.

To quantify MAP2 and GFAP, three z-stacks were taken per section for five sections per rat at a resolution of 310 × 310 × 517 nm^3 for MAP2 and 866 × 866 × 767 nm^3 for GFAP. Each z-stack was restored using Scientific Volume Imaging deconvolution software (Huygens Professional 3.4.0) with Classic Maximum Likelihood Estimation and a theoretical point spread function. Spot count and surfaces were calculated for each image, for MAP2 and

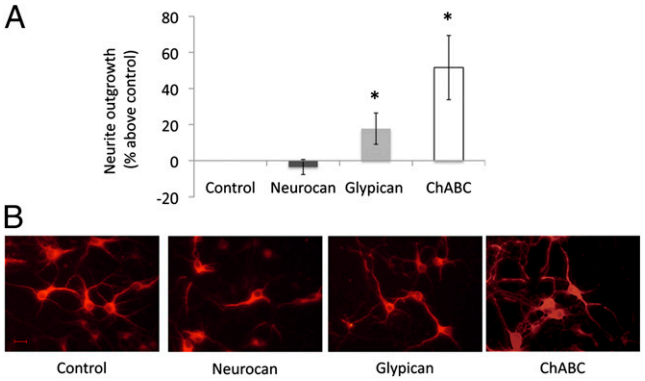

Fig. 5. Effects of extracellular matrix proteins on neurite extension in cortical neuron cultures. E17 primary cortical neuron cultures were plated on a neurite assay kit and treated with PBS (control), neurocan, glypican, or ChABC at the concentrations given in the legend to Fig 4. (*A*) Neurite growth (cresyl violet staining of processes extending across a permeable membrane) was expressed as a mean value ± SEM from three experiments. $*P < 0.05$ compared with control. (*B*) Representative cultures immunostained for MAP2, showing corresponding changes in neurite extension from intact neurons.

GFAP, respectively, using Bitplane Imaris 7.0 software (Bitplane Scientific Software) (44).

Neurobehavioral Testing. Neurobehavioral function was assessed using the ladder rung walking test, cylinder test, and forepaw weakness scale. For the ladder rung walking test, which depends on forelimb and hind-limb stepping, placing and coordination (45), rats were run in the apparatus six times before MCAO to familiarize them with the test and to establish baseline performance. They were assessed on three runs with the number of right forepaw missteps recorded. Ladder rungs were adjusted between trials to prevent habituation. For the cylinder test, which reflects forelimb preference during vertical exploration (46), rats were tested on the day before MCAO to obtain baseline measurements and ensure competency in the test. The cylinder test was performed for 5 min, recording left and right forepaw touches of the cylinder wall. For the forepaw weakness scale, rats were observed concurrently during the cylinder test. One point was given for each sign of weakness (arm drop, wrist drop, finger drop, finger abduction weakness, partial floor limb placement, partial wall contact, dorsal contact of forepaw on floor, and forepaw sliding on floor or wall), with a maximum (most impaired) score of 8 (Fig. S1).

Cell Culture. Cortical neuronal cultures were prepared from embryonic day 17 Sprague–Dawley rat pups (Charles River) (24, 47). Isolated cortex was incubated at 37 °C in Ca^{2+}- and Mg^{2+}-free Earle's balanced salt solution containing 0.001% trypsin 1:250. After 10 min, 10% horse serum was added. Cells were placed in 2 mL of fresh MEM and triturated. Cells were resuspended in Eagle's MEM prepared without glutamine and with twice the usual concentration of vitamins (MEM-Pak; Cell Culture Facility, University of California, San Francisco, CA). On the first DIV, cells were supplemented with glucose (final concentration, 30 mM), 2 mM glutamine, and 15 mM Hepes (pH 7.4). Cell suspensions were filtered through a 70-μm Falcon nylon cell strainer, supplemented with 10% horse serum and 10% FBS, and seeded at 3×10^5 cells per well on 24-well Corning culture dishes coated with 100 μg/mL poly-D-lysine. Cultures were incubated for 20 min at 37 °C in humidified 95% air/5% CO_2, and one-half of the medium was replaced with medium containing 5% horse serum and 5% FBS.

Western Blotting. Protein was extracted with lysis buffer containing 1% Nonidet P-40, 0.5% sodium deoxycholate, 0.1% SDS, 1 μg/mL aprotinin, and 100 μg/mL phenylmethylsulfonyl fluoride. Protein concentration was determined using a Bio-Rad protein assay (Bio-Rad). Western blotting was performed as described previously (48), using mouse anti-MAP2 (1:500; Chemicon), mouse anti-neurocan (1:500; Sigma), rabbit anti-FGF2 (1:350; Santa Cruz Biotechnology), mouse anti-actin (1:2,000; Sigma), and rabbit anti-BDNF (1:200; Santa Cruz Biotechnology). The secondary antibodies were HRP-conjugated anti-mouse (for monoclonal) or anti-rabbit (for polyclonal) IgG (both 1:3,000; Santa Cruz Biotechnology). Peroxidase activity was visualized with a chemiluminescence substrate system (NEN Life Science Probes).

Neurite Growth. Neurite outgrowth was assayed using a commercially available kit (Chemicon) as described previously (24, 25). Neurons were plated at 2×10^5 cells per well on membranes of Costar Transwell cell culture inserts coated with 10 μg/mL laminin and collagen I. Neurons were cultured for 4 d with Neurobasal medium (Invitrogen) and treated with PBS, neurocan (5 μg/mL; Sigma), glypican (5 μg/mL; Sigma), or ChABC (2U/mL; Sigma). Inserts were removed from wells and membranes were gently rinsed with PBS and fixed in ice-cold methanol for 20 min at room temperature. Membranes were then stained with cresyl violet. Cell bodies were removed from membranes with a cotton swab. Cresyl violet was extracted from the retained neurites with 25% 0.2 M acetate buffer (pH 4.5) and 50% reagent alcohol and quantified by absorbance at 562 nm. Each treatment condition was replicated in three wells and the neurite assay was repeated three times.

Data Analysis. Results are reported as means ± SEM from 5 or, for behavioral studies, 10 animals per group. The significance of differences between means was assessed by Student *t* test with $P < 0.05$ considered statistically significant.

ACKNOWLEDGMENTS. This work was supported by National Institutes of Health Grants NS44921 and NS62414 (to D.A.G.) and T32 AG000266 (to J.J.H.).

1. Fawcett JW, Asher RA (1999) The glial scar and central nervous system repair. *Brain Res Bull* 49:377–391.
2. Yiu G, He Z (2006) Glial inhibition of CNS axon regeneration. *Nat Rev Neurosci* 7: 617–627.
3. Deguchi K, et al. (2005) Expression of neurocan after transient middle cerebral artery occlusion in adult rat brain. *Brain Res* 1037:194–199.
4. Rhodes KE, Fawcett JW (2004) Chondroitin sulphate proteoglycans: Preventing plasticity or protecting the CNS? *J Anat* 204:33–48.
5. Rolls A, Shechter R, Schwartz M (2009) The bright side of the glial scar in CNS repair. *Nat Rev Neurosci* 10:235–241.
6. Fitch MT, Silver J (1997) Activated macrophages and the blood-brain barrier: Inflammation after CNS injury leads to increases in putative inhibitory molecules. *Exp Neurol* 148:587–603.
7. Panickar KS, Norenberg MD (2005) Astrocytes in cerebral ischemic injury: Morphological and general considerations. *Glia* 50:287–298.
8. Properzi F, Asher RA, Fawcett JW (2003) Chondroitin sulphate proteoglycans in the central nervous system: Changes and synthesis after injury. *Biochem Soc Trans* 31: 335–336.
9. Coles CH, et al. (2011) Proteoglycan-specific molecular switch for RPTPσ clustering and neuronal extension. *Science* 332:484–488.
10. Silver J, Miller JH (2004) Regeneration beyond the glial scar. *Nat Rev Neurosci* 5: 146–156.
11. Galtrey CM, Fawcett JW (2007) The role of chondroitin sulfate proteoglycans in regeneration and plasticity in the central nervous system. *Brain Res Brain Res Rev* 54: 1–18.
12. Nakamae T, et al. (2010) The effects of combining chondroitinase ABC and NEP1-40 on the corticospinal axon growth in organotypic co-cultures. *Neurosci Lett* 476: 14–17.
13. Moon LD, Asher RA, Rhodes KE, Fawcett JW (2001) Regeneration of CNS axons back to their target following treatment of adult rat brain with chondroitinase ABC. *Nat Neurosci* 4:465–466.
14. Corvetti L, Rossi F (2005) Degradation of chondroitin sulfate proteoglycans induces sprouting of intact purkinje axons in the cerebellum of the adult rat. *J Neurosci* 25: 7150–7158.
15. Bradbury EJ, et al. (2002) Chondroitinase ABC promotes functional recovery after spinal cord injury. *Nature* 416:636–640.
16. García-Alías G, Barkhuysen S, Buckle M, Fawcett JW (2009) Chondroitinase ABC treatment opens a window of opportunity for task-specific rehabilitation. *Nat Neurosci* 12:1145–1151.
17. Nandini CD, et al. (2004) Structural and functional characterization of oversulfated chondroitin sulfate/dermatan sulfate hybrid chains from the notochord of hagfish. Neuritogenic and binding activities for growth factors and neurotrophic factors. *J Biol Chem* 279:50799–50809.
18. Properzi F, et al. (2008) Heparan sulphate proteoglycans in glia and in the normal and injured CNS: Expression of sulphotransferases and changes in sulphation. *Eur J Neurosci* 27:593–604.
19. Tisay KT, Key B (1999) The extracellular matrix modulates olfactory neurite outgrowth on ensheathing cells. *J Neurosci* 19:9890–9899.
20. Jain A, McKeon RJ, Brady-Kalnay SM, Bellamkonda RV (2011) Sustained delivery of activated Rho GTPases and BDNF promotes axon growth in CSPG-rich regions following spinal cord injury. *PLoS ONE* 6:e16135.
21. Kurihara D, Yamashita T (2012) Chondroitin sulfate proteoglycans downregulate spine formation in cortical neurons by targeting tropomyosin-related kinase B (TrkB). *J Biol Chem* 287:13822–13828.
22. Nurcombe V, Ford MD, Wildschut JA, Bartlett PF (1993) Developmental regulation of neural response to FGF-1 and FGF-2 by heparan sulfate proteoglycan. *Science* 260: 103–106.

23. Su G, et al. (2006) Glypican-1 is frequently overexpressed in human gliomas and enhances FGF-2 signaling in glioma cells. *Am J Pathol* 168:2014–2026.
24. Jin K, Mao XO, Greenberg DA (2006) Vascular endothelial growth factor stimulates neurite outgrowth from cerebral cortical neurons via Rho kinase signaling. *J Neurobiol* 66:236–242.
25. Smit M, Leng J, Klemke RL (2003) Assay for neurite outgrowth quantification. *Biotechniques* 35:254–256.
26. Harris NG, Mironova YA, Hovda DA, Sutton RL (2010) Chondroitinase ABC enhances pericontusion axonal sprouting but does not confer robust improvements in behavioral recovery. *J Neurotrauma* 27:1971–1982.
27. Soleman S, Yip PK, Duricki DA, Moon LD (2012) Delayed treatment with chondroitinase ABC promotes sensorimotor recovery and plasticity after stroke in aged rats. *Brain* 135:1210–1223.
28. Hunanyan AS, et al. (2010) Role of chondroitin sulfate proteoglycans in axonal conduction in Mammalian spinal cord. *J Neurosci* 30:7761–7769.
29. Massey JM, et al. (2006) Chondroitinase ABC digestion of the perineuronal net promotes functional collateral sprouting in the cuneate nucleus after cervical spinal cord injury. *J Neurosci* 26:4406–4414.
30. Sato Y, et al. (2008) Reduction of brain injury in neonatal hypoxic-ischemic rats by intracerebroventricular injection of neural stem/progenitor cells together with chondroitinase ABC. *Reprod Sci* 15:613–620.
31. McKeon RJ, Schreiber RC, Rudge JS, Silver J (1991) Reduction of neurite outgrowth in a model of glial scarring following CNS injury is correlated with the expression of inhibitory molecules on reactive astrocytes. *J Neurosci* 11:3398–3411.
32. Kirkham DL, et al. (2006) Neural stem cells from protein tyrosine phosphatase sigma knockout mice generate an altered neuronal phenotype in culture. *BMC Neurosci* 7: 50.
33. Shen Y, et al. (2009) PTPsigma is a receptor for chondroitin sulfate proteoglycan, an inhibitor of neural regeneration. *Science* 326:592–596.
34. Meathrel K, Adamek T, Batt J, Rotin D, Doering LC (2002) Protein tyrosine phosphatase sigma-deficient mice show aberrant cytoarchitecture and structural abnormalities in the central nervous system. *J Neurosci Res* 70:24–35.
35. Xu J, et al. (2010) Effect of chondroitinase ABC on growth associated protein 43 and glial fibrillary acidic protein after spinal cord injury in rats. *Zhongguo Xiu Fu Chong Jian Wai Ke Za Zhi* 24:1212121–1212126.
36. Nudo RJ (2007) Postinfarct cortical plasticity and behavioral recovery. *Stroke* 38(2 Suppl):840–845.
37. Walicke P, Cowan WM, Ueno N, Baird A, Guillemin R (1986) Fibroblast growth factor promotes survival of dissociated hippocampal neurons and enhances neurite extension. *Proc Natl Acad Sci USA* 83:3012–3016.
38. Irving EA, et al. (2005) Identification of neuroprotective properties of anti-MAG antibody: A novel approach for the treatment of stroke? *J Cereb Blood Flow Metab* 25: 98–107.
39. Seymour AB, et al. (2005) Delayed treatment with monoclonal antibody IN-1 1 week after stroke results in recovery of function and corticorubral plasticity in adult rats. *J Cereb Blood Flow Metab* 25:1366–1375.
40. Suzuki T, et al. (2007) Chondroitinase ABC treatment enhances synaptogenesis between transplant and host neurons in model of retinal degeneration. *Cell Transplant* 16:493–503.
41. Karimi-Abdolrezaee S, Eftekharpour E, Wang J, Schut D, Fehlings MG (2010) Synergistic effects of transplanted adult neural stem/progenitor cells, chondroitinase, and growth factors promote functional repair and plasticity of the chronically injured spinal cord. *J Neurosci* 30:1657–1676.
42. Jin K, et al. (2010) Transplantation of human neural precursor cells in Matrigel scaffolding improves outcome from focal cerebral ischemia after delayed postischemic treatment in rats. *J Cereb Blood Flow Metab* 30:534–544.
43. Nawashiro H, Tasaki K, Ruetzler CA, Hallenbeck JM (1997) TNF-alpha pretreatment induces protective effects against focal cerebral ischemia in mice. *J Cereb Blood Flow Metab* 17:483–490.
44. Bacigaluppi M, et al. (2009) Delayed post-ischaemic neuroprotection following systemic neural stem cell transplantation involves multiple mechanisms. *Brain* 132: 2239–2251.
45. Metz GA, Whishaw IQ (2002) Cortical and subcortical lesions impair skilled walking in the ladder rung walking test: A new task to evaluate fore- and hindlimb stepping, placing, and co-ordination. *J Neurosci Methods* 115:169–179.
46. Schallert T, Fleming SM, Leasure JL, Tillerson JL, Bland ST (2000) CNS plasticity and assessment of forelimb sensorimotor outcome in unilateral rat models of stroke, cortical ablation, parkinsonism and spinal cord injury. *Neuropharmacology* 39: 777–787.
47. Jin K, et al. (2001) Caspase-3 and the regulation of hypoxic neuronal death by vascular endothelial growth factor. *Neuroscience* 108:351–358.
48. Jin KL, Mao XO, Greenberg DA (2000) Vascular endothelial growth factor: Direct neuroprotective effect in in vitro ischemia. *Proc Natl Acad Sci USA* 97:10242–10247.